electronics

MDPI

Article

Enhancing Small-Cell Capacity with Wireless Backhaul

Ran Tao [1,*] and Wuling Liu [2]

[1] Department of Electronics and Information Engineering, Nanjing University of Information Science and Technology, Nanjing 210044, China
[2] Aerospace Information Research Institute, Chinese Academy of Sciences, Beijing 100094, China; liuwuling@aircas.ac.cn
* Correspondence: 003339@nuist.edu.cn

Abstract: Recently, hyperdense small cells have been proposed to meet the challenge of the tremendous increment in cellular data service requirements. To reduce the deployment cost, as well as operated cost, these small cells are usually connected to limited backhauls, in which case the backhaul capacity may become a bottleneck in busy hours. In this paper, we propose an optimal scheme for the small cells to utilize the macrocell links as its wireless backhaul. Based on stochastic geometry, the analytical expressions of network capacity with in-band and out-band wireless backhaul are derived and validated using simulation results. The optimized results show that our proposed scheme can significantly improve the network performance in scenarios with a high traffic load.

Keywords: UAV; intelligent reflecting surface; stochastic geometry; HetNet

Citation: Tao, R.; Liu, W. Enhancing Small-Cell Capacity with Wireless Backhaul. *Electronics* **2024**, *13*, 797. https://doi.org/10.3390/electronics13040797

Academic Editor: Adão Silva

Received: 22 January 2024
Revised: 11 February 2024
Accepted: 14 February 2024
Published: 19 February 2024

1. Introduction

To address the explosive growth in data demands driven by mobile phones, network operators will have to significantly increase the capacity of their networks. The deploymentof dense small cells has been considered as a key technology to offer high throughput and contentious coverage [1]. However, sometimes, the small cells connect to the core network by low capacity backhaul (e.g., DSL links), in which case the backhaul capacity may become a bottleneck in busy hours and the QoS of UEs cannot be guaranteed [2]. The wireless backhaul for small cells can be a desirable solution because it is cheaper and more flexible compared with fiber backhaul [3].

In [4], the authors proposed three strategies of a small-cell in-band wireless backhaul in massive MIMO systems to achieve throughput increase. However, they do not consider the intercell interference; moreover, the original backhaul capacity and the influence of user density on the macrocell performance are not mentioned in the paper. In [5], the authors maximize network energy efficiency by allocating both the transmission power of each small-cell base station to users and bandwidth for backhauling. In [6], the cell-planning problem for a two-tier network containing the BSs with a fiber backhaul and BSs with a wireless backhaul is investigated. The authors propose an algorithm to determine the minimum number of wired-BS and wireless-BS to satisfy the given cell and capacity coverage constraints. In [7], considering ultra-dense small-cell networks with optical and wireless backhaul, the authors design an energy-efficient backhauling strategy and propose a heuristic solution to solve the problem. In [8], the authors maximize the sum rate of a self-backhauled full-duplex dense, small-cell network under quality-of-service requirements and backhaul capacity constraints. In [9], a power-efficient full-duplex self-backhauling scheme for small cells of cellular networks is proposed, and the authors jointly optimize the backhaul link TX powers for multiple small cells while maintaining the same UE capacity. All the aforementioned works focus on the optimization of network performance with the wireless backhaul. In [10–12], the network capacity performance with a wireless backhaul was evaluated analytically. In [10], the authors analyze the self-backhauling in as band

full duplex HetNets architecture using a stochastic geometry-based model. However, the authors do not consider the original backhaul capacity. In [11], the authors provide a minimum average hop number algorithm to optimize the network capacity and energy efficiency. In [12], the upper bound of the network capacity with wireless backhaul is evaluated based on the number of antennas per BS. In [13], with the tool of stochastic geometry, the authors examine the performance of mMTC in an ultra-dense network (UDN) environment that utilizes the mmWave band and employs wireless backhaul support for the small cell. In [14], the authors propose a load-balancing algorithm for small-cell-integrated access and backhaul networks operating in the millimeter wave (mmWave) band. The simulation results show that the proposed algorithm not only distributes the load across small cells more evenly but also increases network capacity. In [15], the authors jointly optimize the user association and backhaul resource allocation in mmWave HetNets, and a multi-agent deep reinforcement-learning-based scheme is proposed to maximize the long-term total link throughput of the network. In [16], the authors propose a multi-agent distributed Q-learning algorithm with pre-resource partitioning to solve the problem of channel allocation and energy consumption of integrated access and backhaul networks. In [17], the authors jointly optimize transmission precoding and rate allocation to maximize the spectral efficiency in rate-splitting multiple access HetNets.

In this paper, a scheme that uses macrocell link as a wireless backhaul for small cells to maximize the capacity of the entire network is proposed. Both out-band frequency division duplex (OB-FDD) and in-band full duplex (IB-FD) approaches are used to verify the proposed maximization. To the best of our knowledge, the numerical performance evaluation in terms of network throughput with various numbers of users of each cell under a limited backhaul scenario has not yet been provided.

The capacity enhancement with wireless backhaul is evaluated in terms of two aspects. (1) The capacity of the target small cell A, which has a distance D from the macrocell, is analyzed, which can be seen in Figure 1. In reality, it is worth noting that the network operators will come across a situation in which the traffic of certain areas has a significant increase, rather than the whole area, and the wireless backhaul only needs to be provided to the small cells in these areas. Therefore, it is quite meaningful to analyze the capacity of certain small cells with wireless backhaul. (2) The throughput of the whole network is analyzed, including the macrocell and all small cells. The system model is illustrated in Figures 2 and 3. Most of the papers in this area target the optimization of UEs' coverage probability, but the studies about network throughput performance evaluation are insufficient. In this part, a detailed analysis of the network throughput is proposed.

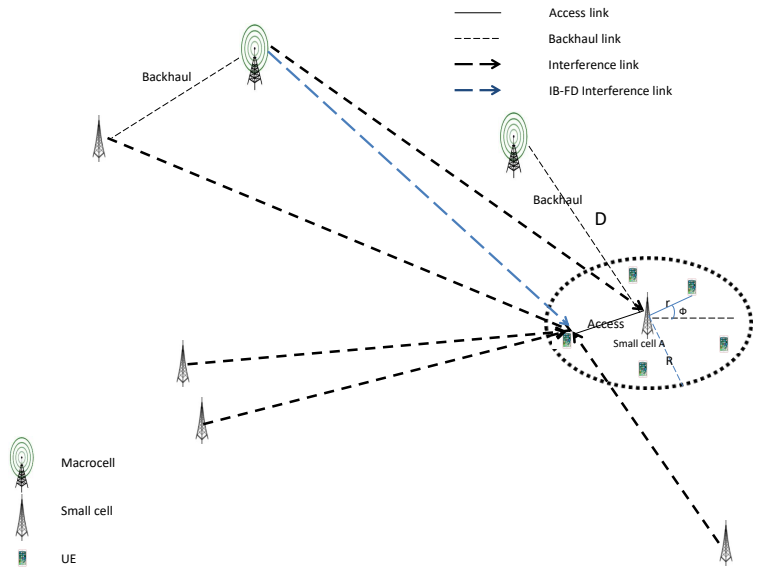

Figure 1. Capacity analysis of small cell A.

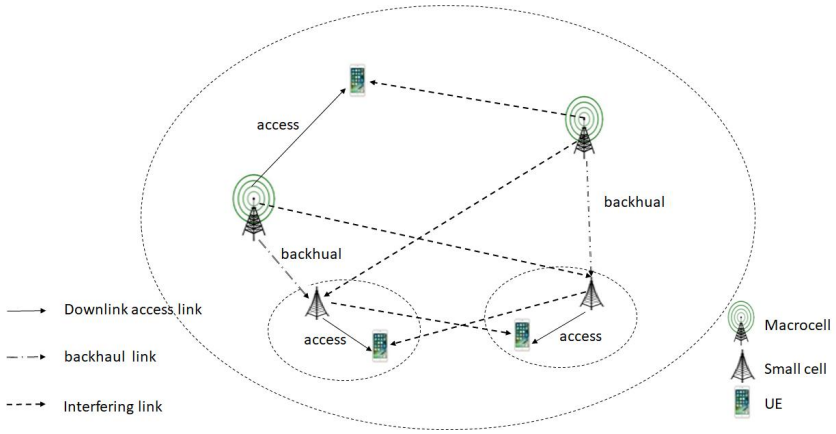

Figure 2. OB-FDD system model.

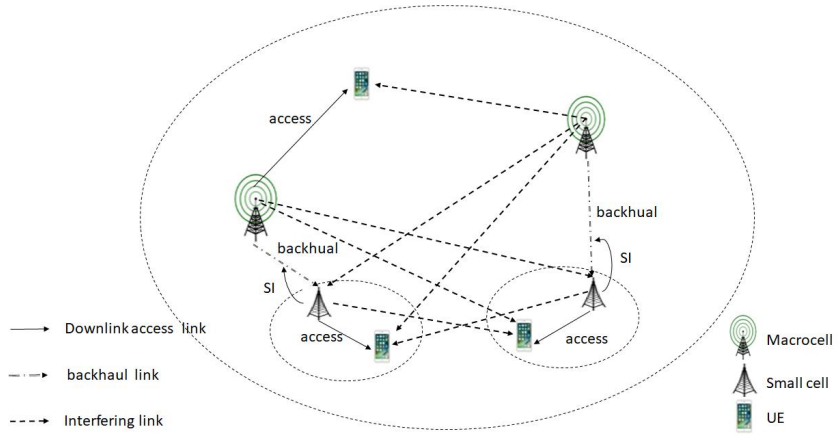

Figure 3. IB-FD system model.

2. System Model

In OB-FDD networks, wireless resources allocated to links between the macrocell and small cells are orthogonal to those allocated for the data exchange between the small cell and its associated UEs, as shown in Figure 2. On the other hand, in IB-FD networks, small cells are able to carry out self-interference cancellation. Therefore, IF-FD is able to transmit and receive signals in the same time–frequency resource, as shown in Figure 3. For the IB-FD system model, we can see that there are two types of interference: (1) the self-interference(SI) at the small cells and (2) the backhaul interference to the UEs. It is noted that due to internal buffering and processing delay of the SBS receiver circuitry, the transmitted signal (i.e., signal from small cells to UEs) and received signal (i.e., the signal from macrocells to small cells) may not necessarily be the same. In that case, the interference from the small cells to the backhaul link can be removed [18].

The system model consists of both macrocells and small cells deployed according to a homogeneous Spatial Poisson Point Process (SPPP) Φ with intensity λ_1 and λ_2, respectively, in the Euclidean plane. The UEs are uniformly distributed within the entire area. The backhaul capabilities for the macrocells are assumed to be profound, and the small cells are connected to limited backhauls. W denotes the whole bandwidth of the network. In the small cell, the spectrum is divided into subchannels, each with bandwidth b. Suppose that N represents the number of available sub-channels in the network; if N servers are all busy simultaneously, then any new arrival requests would be dropped.

We assume that the transmitter and the receiver experience Rayleigh fading with a mean of 1 and employ a constant transmit power of $1/\mu$. A similar assumption has been

made in [19]. In this case, the received power at a typical receiver at a distance d from its transmitter can be written as

$$g = d^{-\alpha}\|h\|^2, \tag{1}$$

where α is the path loss distance exponent, and we assume that the path loss exponent for macroell and small cell is the same: $\alpha_s = \alpha_m = \alpha$. d is the distance between the transmitter and receiver, where α is the path loss distance exponent and h follows an exponential distribution with mean $1/\mu$, which we denote as $h \sim \exp(\mu)$. The central carrier frequency is set to 2.4 GHz in this paper.

For a typical UE l associated with a BS in tier k, its SINR Y_l is

$$\mathrm{Y}_l = \frac{g_{l,0}P_k}{\sum_{j=1}^{K}\sum_{i\in\mathcal{C}_j\setminus B_{k0}} g_{l,i}P_j + \sigma^2}, \tag{2}$$

where $P_k, k = s \; or \; m$ is the transmit power of the serving BS, $g_{i,0}$ and $g_{jl,i}$ are the channel gain (as defined in (1)) of the link from the serving BS to the UE l and the interfering links to the UE l, respectively; $\mathcal{C}_j$ is the set of BSs; and σ^2 is the additive white Gaussian noise (AWGN) power.

The SINR Y_m for the link between macrocell BS and the small-cell BS is

$$\mathrm{Y}_m = \frac{g_{m,0}P_m}{\sum_{j=1}^{K}\sum_{i\in\mathcal{C}_j\setminus B_{m0}} g_{s,i}P_j + \sigma^2}, \tag{3}$$

where P_m is the transmission power of the macrocell, $g_{s,0}$ is the channel gain of the link from the macro BS to the target small cell, and $g_{s,i}$ values are the channel gain (as defined in (1)) of interfering links from other BSs to the target small cell. $\mathcal{C}_j$ is the set of interfering BSs.

In this paper, we consider the Shannon capacity. R_i is the capacity of UE i. At time t, the number of total requests of a small cell is $N(t)$, and thus, the total throughput (bits/s) of a small cell is

$$R_T = \sum_{i=0}^{N(t)} R_i = \sum_{i=0}^{N(t)} b\log_2(1+\mathrm{Y}_i) \tag{4}$$

We consider a transmission time period T ($T \gg T_c$). We assume that perfect interleaving is fulfilled under certain coherence time and delay restrictions, the receiver has a perfect Channel Quality Indicator, and the fading channel can be transformed into an equivalent stochastic channel model, which is a strong stationary process [20]. Thus, we can use the ergodic capacity to represent the statistical expectation of the Shannon capacity over all fading states.

We suppose that at time t, there are $\rho(t)$ UEs that come into the coverage of the small cell A, and the number of available channels is expressed as N. The mean number of UEs served by the small cell can be expressed as

$$\mathbb{E}[N(t)] = \min(\rho(t), N). \tag{5}$$

As each small cell is connected to a limited backhaul, its backhaul capacity C_b might not be enough to sustain the total capacity R_C required of its radio access links, i.e., $C_b < R_C$. Therefore, we use τB for a wireless backhaul with macro-BS ($0 \leq \tau \leq 1$). It is also noted that the macrocell also needs to serve its UEs. The bandwidth that can be used for the communication between the macro BS and small cells is τB for the out-band frequency division duplex (OB-FDD) method and B for the in-band full duplex (IB-FD) method. Thus, for a specific τ, we have $N = \lfloor (1-\tau)B/b \rfloor$ for OB-FDD and $N = \lfloor B/b \rfloor$ for IB-FD. Here, b is the number of channels a user occupies. The average backhaul capacity the macro cell provides can be modeled as its ergodic capacity [4,21]. It is noted that for OB-FDD, the wireless backhaul is only interfered with by other macrocells; however, for IB-FD, the wireless backhaul receives interference from both tiers.

2.1. Performance Analysis

2.1.1. Capacity Analysis of the Target Small Cell

In this part, the capacity of a target small cell utilizing the wireless backhaul from a macrocell will be analyzed first. Without a loss of generality, the distance between the chosen macrocell and small cell A is set to D. This is quite meaningful as sometimes the macrocell will only communicate with certain small cells to provide wireless backhaul. The OB-FDD method and the IB-FD method are compared in this section. Figure 1 is used to illustrate the analysis.

The capacity (C_m) of the wireless backhaul from the macrocell to small cell A can be expressed as follows.

Theorem 1. *The ergodic capacity C_m is*

$$\begin{aligned} C_m =& B\left(\mathbb{E}\left(log_2\left(1+\frac{P_m h D^{-\alpha_m}}{I_s+I_m+\sigma^2}\right)\right)\right) \\ =& B\left(\int_{t>0}\mathbb{P}\left[log_2(1+\frac{P_m h D^{-\alpha_m}}{I_s+I_m+\sigma^2})>t\right]\mathrm{d}t\right) \\ =& B\left(\int_{t>0}\mathbb{P}\left[h>D^{\alpha_m}P_m(\sigma^2+I_m+I_s)(2^t-1)\right]\mathrm{d}t\right) \\ =& B\left(\int_{t>0}\mathbb{E}(exp(-\frac{\mu D^{\alpha_m}}{P_m}(\sigma^2+I_m+I_s)(2^t-1))\,\mathrm{d}t\right) \\ =& B\left(\int_{t>0}e^{-\sigma^2\mu D^{\alpha_m}T}\mathcal{L}_{I_s}(\mu D^{\alpha_m}T)\mathcal{L}_{I_m}(\mu D^{\alpha_m}T)\,\mathrm{d}t\right), \end{aligned} \tag{6}$$

where $T=\frac{(2^t-1)}{P_m}$. $\mathcal{L}_{I_m}(\mu T D^{\alpha_m}) = exp\left(-\pi\lambda_1 D^2(T*P_m)^{\frac{2}{\alpha_m}}*(\pi/2-atan((T*P_m)^{-\frac{2}{\alpha_m}}))\right)$. *For the OB-FDD approach, as the backhaul link and data links of small cells are in separate frequencies, the backhaul link is freed from the interference of small cells. In that case,* $\mathcal{L}_{I_s}(\mu T D^{\alpha_m})=1$. *For the IB-FD approach, because the backhaul link and data links of small cells share the same frequency band, the backhaul link suffers from interference from small cells. Hence,* $\mathcal{L}_{I_s}(\mu T D^{\alpha_m}) = exp\left(-\pi\lambda_s D^2(T*P_s)^{2/\alpha_s}*(\pi/2)\right)$. $\mu=1$ *is the parameter of exponential fading. The parameters* σ^2, P_s, P_m, *and* λ_s *can be found in Table 1.*

Let $\tau \in [0,1]$ denote the transmission bandwidth fraction required from the macrocell to small cells; then, the downlink capacity of wireless backhaul from the macrocell to the target small cell can be written as:

$$c_m = \tau * C_m, \tag{7}$$

where C_m is expressed in (6), and $\tau=1$ for the IB-FD method.

Then, the ergodic capacity of a UE from small cell A will be calculated. Assume that there are UEs continuously coming into the coverage area of small cell A. Without loss of generality, it is assumed that all these UEs are distributed uniformly in a circle inside the coverage of A with radius R_A. Here, for convenience, an approximation of the range of R will be provided. Firstly, the UEs inside the coverage area will not be associated with the macrocell, that is to say, $P_m * D^{-\alpha_m} < P_s * R_A^{-\alpha_s}$, and it can be derived that $R_A < \frac{P_s}{P_m}^{\frac{1}{\alpha_s}} D^{\frac{\alpha_m}{\alpha_s}}$. (For convenience, it is assumed that the distance between the macrocell and UEs in the small cell A is D.) Secondly, the UEs inside the coverage area will not connect to other small cells. Given that the small cell density is λ_s, the average distance between the two closest small cells is $\frac{1}{2\sqrt{\lambda_s}}$. Therefore, R_A can be approximated as $R_A = min(\frac{1}{2\sqrt{\lambda_s}}, \frac{P_s}{P_m}^{\frac{1}{\alpha_s}} D^{\frac{\alpha_m}{\alpha_s}})$

Theorem 2. *The ergodic capacity of a UE from small cell A* $\mathbb{E}[R_i]$ *can be approximated as*

$$\begin{aligned}\mathbb{E}[R_i] &= \mathbb{E}[log_2(1+SINR)] \\ &= \int_0^{2\pi}\int_0^{R_A} \mathbb{E}[log_2(\frac{P_s h r^{-\alpha_s}}{I_s+I_m+I_{mD}+\sigma^2}]r\,\mathrm{d}r\mathrm{d}\phi \\ &= \int_0^{2\pi}\int_0^{R_A}\int_{t>0} \mathbb{P}[log_2(\frac{P_s h r^{-\alpha_s}}{I_s+I_m+I_{mD}+\sigma^2} > t]\,\mathrm{d}t r\mathrm{d}r\mathrm{d}\phi \\ &= \int_0^{2\pi}\int_0^{R_A}\int_{t>0} \mathbb{E}(e^{-\mu r^{\alpha_s}(\sigma^2+I_s+I_m+I_{mD})(2^t-1)/P_s})\,\mathrm{d}t r\mathrm{d}r\mathrm{d}\phi \\ &= \int_0^{2\pi}\int_0^{R_A}\int_{t>0} e^{-\mu r^{\alpha_s}(\sigma^2+I_{mD})(2^t-1)/P_s}\mathcal{L}_{I_s}(\mu r^{\alpha_s}(\frac{2^t-1}{P_s}))\mathcal{L}_{I_m}(\mu r^{\alpha_s}(\frac{2^t-1}{P_s}))\,\mathrm{d}t r\mathrm{d}r\mathrm{d}\phi, \end{aligned} \tag{8}$$

where ϕ is the angle of the x-axis and the line between small cell A and UE, I_s is the interference from other small cells, I_{mD} is the interference from the macrocell that communicates with small cell A, and I_m is the interference from other macrocells.

The Laplace transform of I_s is

$$\mathcal{L}_{I_s}(\mu r^{\alpha_s}(\frac{2^t-1}{P_s})) = exp\left(-\pi\lambda_2 r^2((\frac{2^t-1}{P_s})*P_s)^{2/\alpha_s} * (\pi/2 - atan(((\frac{2^t-1}{P_s})*P_s)^{-2/\alpha_s}))\right). \tag{9}$$

For IB-FD, I_{mD} can be expressed as

$$I_{mD} = P_m(D^2+r^2-2Drcos(\phi+\pi/2))^{-\alpha_s/2}. \tag{10}$$

The Laplace transform of I_m is

$$\begin{aligned}&\mathcal{L}_{I_m}(\mu r^{\alpha_s}(\frac{2^t-1}{P_s})) \\ &= exp\left(-\pi\lambda_1 r^2((\frac{2^t-1}{P_s})*P_m)^{2/\alpha_m} * (\pi/2 - atan((D/r)^2\cdot(\frac{2^t-1}{P_s})*P_m)^{-2/\alpha_m}))\right).\end{aligned} \tag{11}$$

For OB-FDD, $\mathcal{L}_{I_m}(\mu r^{\alpha_s}(\frac{2^t-1}{P_s})) = 1$. $I_{mD} = 0$.
The parameters μ, σ^2, P_s, and λ_s can be found in Table 1.
The total throughput of the target small cell can be expressed as

$$R_c = \lambda_u \pi R_A^2 \mathbb{E}[R_i], \tag{12}$$

It is noted that for the IB-FD approach, $\tau = 1$ as all bandwidth of the macrocell is utilized as wireless backhaul to support small cell A. Hence, we only need to provide the solution for *the Optimal (OPT)* of FDD method in this section.

Definition 1. *The total capacity of the small cell is defined as*

$$C_\tau = \min\{R_C, C_b + c_m\}. \tag{13}$$

Here, the aim is to maximize the capacity of the small cell

$$\text{OPT:} \qquad \arg\max_{\tau} C_\tau \tag{14}$$

$$\text{s.t.,} \qquad \tau \le \tau^\dagger \tag{15}$$

where $\tau^\dagger = 1$ represents the maximum portion of bandwidth that can be utilized for wireless backhaul.

Proposition 1. *The solution* τ^* *to* OPT *is the solution* τ_s *of the following equation*

$$R_C = C_b + c_m, \tag{16}$$

if $\tau_s \leq \tau^\dagger$ *; otherwise,* $\tau^* = \tau^\dagger$*, where* C_b *is the optical backhaul capacity, and* c_m *is in (7).*

Proof. It is easy to prove that c_m defined in (6) (Theorem 2) strictly increases with τ. In addition, it can be seen that R_C strictly decreases with τ. Thus, when $\tau < \tau_s$, $c_m + C_b < R_C$ and $C_\tau = c_m + C_b$, while $\tau > \tau_s$, $c_m + C_b > R_C$ and $C_\tau = R_C$. It is easy to find that C_τ increases with τ for $\tau \in [0, \tau_s]$ and decreases with τ for $\tau \in [\tau_s, 1]$. With these discussions, we conclude that C_τ reaches its maxima at τ_s. Thus, it is known that $\tau^* = \tau_s$ if $\tau_s < \tau^\dagger$; otherwise $\tau^* = \tau^\dagger$. □

It is worth noting that (16) can be efficiently solved using numerical algorithms, such as Brent's method [22].

Table 1. System parameters.

Macro/Small cell/UE distribution	PPP/PPP/uniform distribution
Density of macrocells (λ_m)	$1.5^{-6}/\mathrm{m}^2$
Density of small cells (λ_s)	$6^{-5}/\mathrm{m}^2$
Bandwidth allocation (W)	10 MHz
Power consumption of macrocells (P_1)	40 W
Power consumption of small cells (P_2)	1 W/2 W
Macro/Small cell pathloss exponent (α_m/α_s)	4
Original wired backhaul (C_b)	2×10^6 Hz, 6×10^6 Hz
Noise power (σ^2) [dbm]	−104
Bandwidth of Resource Block (RB) [Hz]	180 K
Number of subcarriers per RB	12
Bandwidth of subcarrier [Hz]	15 k
parameter of fading channel h (μ)	1

2.1.2. Capacity Analysis of the HetNets with Wireless Backhaul

In this part, we provide a numerical analysis of the network throughput. We make an assumption that the throughput of the small cells can be divided into two groups: (1) Group A: the traffic of the small cell is beyond of the capacity of wired and wireless backhaul. (2) Group B: The traffic of the small cell can still be supported by the wired and wireless backhaul.

In this part, a numerical analysis of the network throughput is provided. We make an assumption that the throughput of the small cells can be divided into two groups: (1) Group A: the traffic of the small cell is beyond the capacity of wireless backhaul. (2) Group B: The traffic of the small cell can still be supported by the wireless backhaul.

The numerical analysis of the throughput of small cells in Group A is as follows:

Lemma 1. *Given a random variable X, and a constant a, then* $\mathbb{E}[X \cdot \mathbf{1}\{x \leq a\}] = a\mathbb{P}\{x \leq a\} - \int_0^a \mathbb{P}\{x \leq t\}\,\mathrm{d}t$

On the basis of Lemma 1, the average throughput $\mathbb{E}[R_A]$ of a small cell in group A can be calculated as

$$\mathbb{E}[R_A] = \mathbb{E}[C_{backhaul}\mathbf{1}\{C_{backhaul} \leq C_S\}], \tag{17}$$

where $C_{backhaul}$ is the average backhaul capacity and can be expressed as

$$C_{backhaul} = W\tau \log 2(1+\gamma) + C_b, \tag{18}$$

where $W\tau \log_2(1+\gamma)$ is the expression of the capacity of the wireless backhaul and C_b is the expression of the capacity of wired backhaul.

C_S is the sum of UEs' data rate of a small cell and can be expressed as

$$C_S = R_s * \mathbb{E}[N_s(t)], \tag{19}$$

where R_s is the average data rate of small cell UEs, which can be found in [23], and the average number of UEs of each small cell is $n_s = \lambda_u * A_2/\lambda_s$. A_2 is the UE association probability of small cells, which can also be found in [23]. Based on (5), the average UEs served by the small cells can be written as $\mathbb{E}[N_s(t)] = \min(n_s, N)$, where N is the number of available channels and is defined in Section 2. According to Lemma 1, (17) can be derived as

$$\begin{aligned}
&\mathbb{E}[R_A] \\
&= \mathbb{E}[C_{backhaul} \cdot \mathbf{1}\{C_{backhaul} \le C_S\}] \\
&= \mathbb{E}[(W_b\tau \log_2(1+\gamma) + C_b) \cdot \mathbf{1}\{W_b\tau \log_2(1+\gamma) + C_b \le R_s * \mathbb{E}[N_s(t)]\}] \\
&\overset{(a)}{=} R_s * \mathbb{E}[N_s(t)] * q_A - \int_0^{R_s * n_s} \mathbb{P}(W_b\tau \log_2(1+\gamma) + C_b \le t)\, \mathrm{d}t,
\end{aligned} \tag{20}$$

where (a) follows Lemma 1. q_A is the probability that a small cell is in group A, which can be written as $q_A = \mathbb{P}\{W_b\tau log2(1+\gamma) + C_b \le R_s * \mathbb{E}[N_s(t)]\}$. γ is the SINR of small cell UEs; for FDD, it can be expressed as $\gamma_F = \frac{P_m r^{-\alpha_m} h}{I_m + \sigma^2}$, and for IB-FD, it can be expressed as $\gamma_Z = \frac{P_m r^{-\alpha_m} h}{I_m + I_s + \sigma^2}$. In this section, the bandwidth is assumed to be equally divided to allocate to each wireless backhaul link therefore, $W_b = \frac{W}{\lambda_s/\lambda_m}$.

q_A can be further derived as

$$\begin{aligned}
q_A &= \mathbb{P}\{W_b\tau log2(1+\gamma) + C_b \le R_s * \mathbb{E}[N_s(t)]\} \\
&= \int_0^{+\infty} (1 - e^{-\sigma^2 \mu r^{\alpha_m} T_1} \mathcal{L}_{I_m}(\mu T_1 r^{\alpha_m}) \\
&\quad * \mathcal{L}_{I_s}(\mu T_1 r^{\alpha_m})) 2\pi\lambda_1 r \exp(-\lambda_1 \pi r^2)\, \mathrm{d}r.
\end{aligned} \tag{21}$$

Based on (20), $\mathbb{E}[R_A]$ can be derived as

$$\begin{aligned}
&\mathbb{E}[R_A] = R_s * \mathbb{E}[N_s(t)] * q_A - \\
&\int_{r>0} \int_0^{R_s * \mathbb{E}[N_s(t)]} (1 - e^{-\sigma^2 \mu r^{\alpha_m} T_2} \mathcal{L}_{I_m}(\mu T_2 r^{\alpha_m}) \\
&* \mathcal{L}_{I_s}(\mu T_2 r^{\alpha_m})) 2\pi\lambda_1 r \exp(-\lambda_1 \pi r^2)\, \mathrm{d}t\, \mathrm{d}r,
\end{aligned} \tag{22}$$

For the FDD approach, $\mathcal{L}_{I_s}(\mu T_2 r^{\alpha_m}) = 1$. For the IB-FD approach, $\mathcal{L}_{I_m}(\mu T_1 r^{\alpha_m})$ and $\mathcal{L}_{I_s}(\mu T_2 r^{\alpha_m})$ can be expressed as

$$\begin{aligned}
&\mathcal{L}_{I_m}(\mu T_1 r^{\alpha_m}) \\
&= \exp\Big(-\pi\lambda_1 r^2 (T_1 * P_m)^{2/\alpha_m} * (\pi/2 - \arctan((T_1 * P_m)^{-2/\alpha_m}))\Big),
\end{aligned} \tag{23}$$

$$\mathcal{L}_{I_s}(\mu T_2 r^{\alpha_m}) = \exp\Big(-\pi\lambda_2 r^2 (T_2 * P_s)^{2/\alpha_m} * (\pi/2))\Big)), \tag{24}$$

where $T_1 = \frac{2^{\frac{R_s * \mathbb{E}[N_s(t)] - Cb}{W_b \tau}} - 1}{P_m}$ ($\tau = 1$ for IB-FD) and $T_2 = \frac{2^{\frac{t - Cb}{W_b \tau}} - 1}{P_m}$.

The total throughput of small cells in group A (T_A) is

$$\begin{aligned} T_A =& \mathbb{E}[R_A] * \mathbb{E}[N_A] \\ =& \mathbb{E}[R_A] * q_A * \lambda_s / \lambda_m, \end{aligned} \tag{25}$$

where $\mathbb{E}[R_A]$ is expressed in (22), q_A is expressed in (21), and $\mathbb{E}[N_A]$ is the number of small cells in group A and is expressed as $\mathbb{E}[N_A] = q_A * \lambda_s / \lambda_m$.

The numerical analysis of the throughput of small cells in Group B is as follows:

Lemma 2. *Given a random variable X and a constant A, then*

$$\begin{aligned} \mathbb{E}[A \cdot \mathbf{1}\{A \leq X\}] &= \mathbb{E}[\mathbb{E}[A \cdot \mathbf{1}\{A \leq X\}|A]] \\ &= \int \mathbb{E}[a\mathbf{1}(a \leq X)] \mathrm{d}P_A(a) \\ &= \int a \cdot \mathbb{P}[a \leq X] \mathrm{d}P_X(x) \end{aligned} \tag{26}$$

According to Lemma 2, the average throughput $\mathbb{E}[R_B]$ of a small cell in group B can be calculated as

$$\begin{aligned} &\mathbb{E}[R_B] \\ &= \mathbb{E}[C_S \cdot \mathbb{P}\{C_{Backhaul} \geq C_S\}] \\ &= \mathbb{E}[R_s \cdot \mathbb{E}[N_s(t)] \cdot \mathbb{P}\{W_b \tau \log_2(1+\gamma) \geq R_s \cdot \mathbb{E}[N_s(t)]\}] \\ &= \int_{d \geq 0} \int_{A \geq 0} R_s \cdot [A\lambda_u] \cdot \exp(F(d,A)) f_d(D) f_a(A) \mathrm{d}d\mathrm{d}A, \end{aligned} \tag{27}$$

where $F(d, A)$ can be expressed as

$$F(d,A) = e^{-\sigma^2 \mu r^{\alpha_m} T_1} \mathcal{L}_{I_m}(\mu T_1 r^{\alpha_m}) \mathcal{L}_{I_s}(\mu T_1 r^{\alpha_m}) 2\pi\lambda_1 r \exp(-\lambda_1 \pi r^2), \tag{28}$$

$\mathcal{L}_{I_m}(\mu T_1 r^{\alpha_m})$ and $\mathcal{L}_{I_s}(\mu T_1 r^{\alpha_m})$ can be found in (23) and (24). The total throughput of small cells in group B (T_B) is

$$\begin{aligned} T_B =& \mathbb{E}[R_B] * \mathbb{E}[N_B] \\ =& \mathbb{E}[R_B] * q_B * \lambda_s / \lambda_m \\ =& \mathbb{E}[R_B] * (1 - q_A) * \lambda_s / \lambda_m \end{aligned} \tag{29}$$

where $\mathbb{E}[R_B]$ is expressed in (27).

Based on (25) and (29), the small cell network total throughput T_s can be derived:

$$\begin{aligned} T_s &= T_A + T_B \\ &= \mathbb{E}[R_A] * \mathbb{E}[N_A] + \mathbb{E}[R_B] * \mathbb{E}[N_B] \\ &= \mathbb{E}[R_A] * q_A * \lambda_s / \lambda_m + C_S * (1 - q_A) * \lambda_s / \lambda_m. \end{aligned} \tag{30}$$

The throughput of the macrocell can be written as $T_m = R_m * \lambda_u * (1 - A_2)/\lambda_1$, where R_m is the average data rate of the macrocell UEs, A_2 is the UE association probability to small cells, the expression of which can be found in [23], and λ_1 is the density of macrocells. Finally, the average total throughput of all the BSs in one macrocell coverage area can be derived as

$$\begin{aligned} T &= T_s + T_m \\ &= T_s + R_m * \mathbb{E}[N_m] \\ &= \mathbb{E}[R_A] * q_A * \lambda_s / \lambda_m \\ &+ C_S * (1 - q_A) * \lambda_s / \lambda_m + R_m * \lambda_u * (1 - A_2)/\lambda_1. \end{aligned} \tag{31}$$

3. Results and Discussion

Based on (6)–(8), (12) and (16), the maximum capacity of small cell A can be derived. The values of all the parameters used in the simulation can be found in Table 1. A brief introduction of the simulation used in this paper will be provided. Matlab is used as the simulation tool. In the simulation, the small cells, as well as UEs, are distributed in a circle area with a radius of 500 m, and the macrocell is deployed at the center of the area. The small cells follow an SPPP distribution with a density of $6 \times 10^{-5}/\mathrm{m}^2$. The received power in the simulation is written in the form $P_r = P_t * K * \frac{d}{d_0}^{-\alpha} * h$, where P_t is the BS transmission power, K and d_0 are set to be 1, and h is the Rayleigh fading and can be generated with '$exprnd$' function. The values of all the parameters used in the simulation can be found in Table 1. In the simulation, the actual throughput of the small cell can be obtained from (16) in the paper, where $C_b + c_m$ is the backhaul capacity of the small cell, and R_c is the UEs' capacity of the small cell. It is noted that the Monte Carlo method is used in the simulation, and the loop count is 100,000 times.

Figures 4 and 5 can be obtained from the optimization of (16). Both figures illustrate the capacity of small cell A with the OB-FDD and IB-FD methods. It can be seen that the OB-FDD method outperforms the IB-FD method significantly, which is for two reasons: (1) With the IB-FD method, the spectrum efficiency of UEs' data links and wireless backhaul links degrade on a large scale due to the cross-tier interference. (2) For the OB-FDD method, the whole spectrum can be utilized to communicate with small cell A ($\tau^{\dagger} = 1$), especially when the UE density is low, which means enough bandwidth can be allocated to small cell A as its wireless backhaul link to serve its traffic. Furthermore, it is obvious to see that both OB-FDD and IB-FD achieve much better performance than the original baseline. In addition, the enhancement of the wireless backhaul falls with the increase in D.

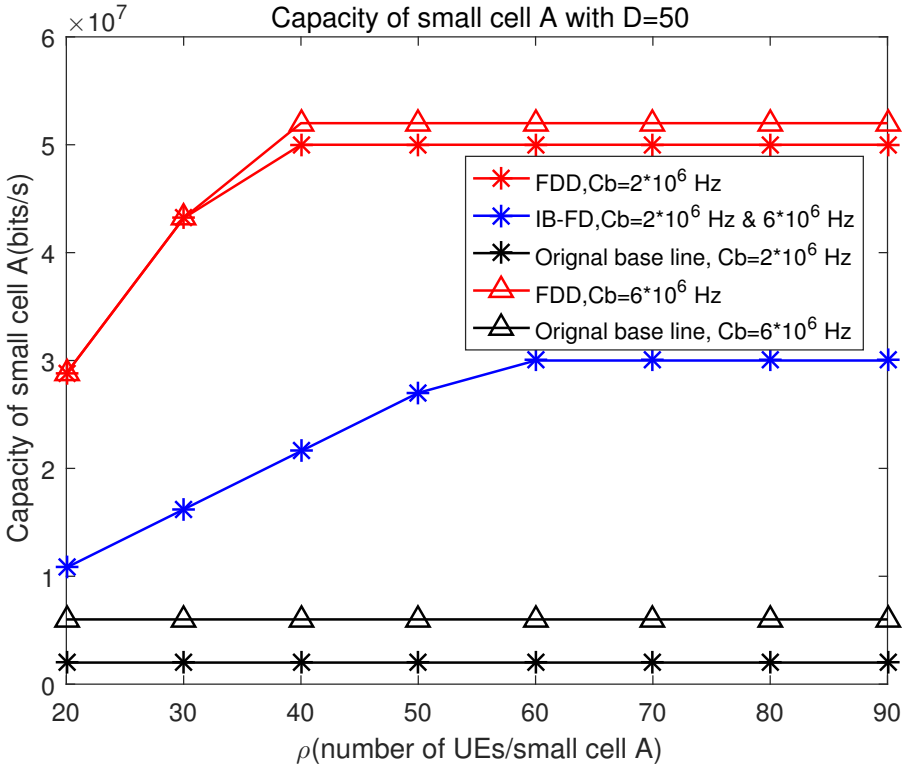

Figure 4. Capacity of small cell A with D = 50.

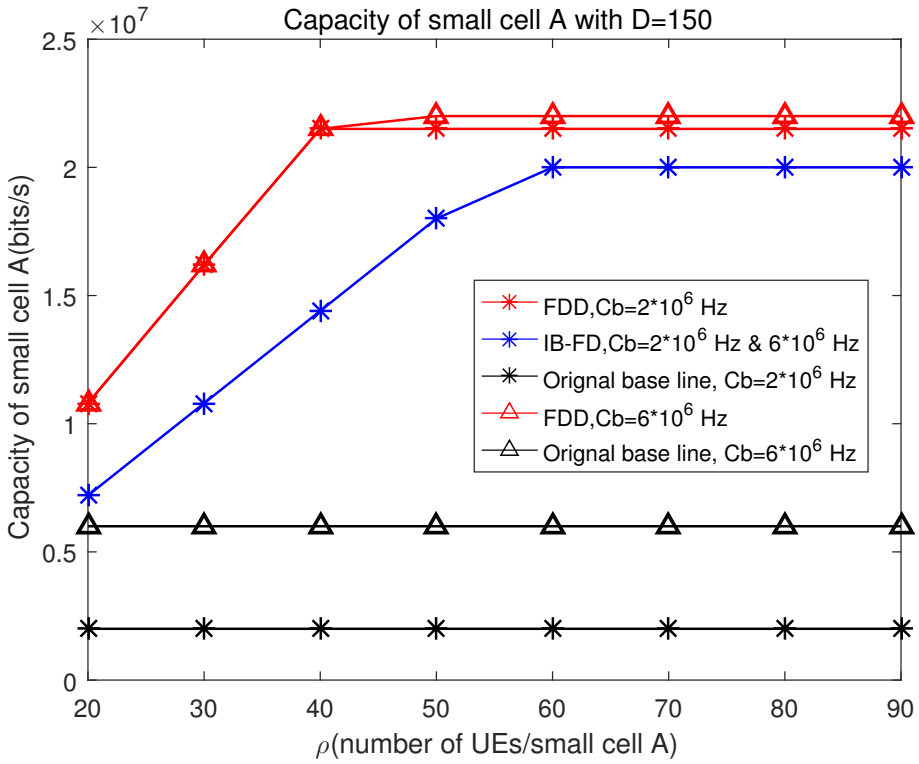

Figure 5. Capacity of small cell A with D = 150.

The capacity of the HetNet with wireless backhaul will also be analyzed in this section based on (25), (29) and (31).

Figures 6 and 7 depict the relationship of the OB-FDD network throughput (in a macrocell coverage) with a given α. redThe scattered points represent the simulation results, and we omit the simulation legends due to the space limits. It is obvious that the throughput of the network decreases rapidly when α is quite large, which is because only a small number of resources are left for small cells and can serve quite a few UEs. When comparing both figures, we can see that the small-cell network's throughput increases with an increase in C_b. Moreover, the improvement in throughput of $P_2 = 2W$ is more significant than that with the OB-FDD approach because IB-FD utilizes the whole bandwidth to serve UEs. It also can be seen that the network performance has only a slight difference with $P_2 = 2W$, compared with that of $P_2 = 1W$. The reason is that due to the backhaul and available channel limits, the number of UEs associated with small cells will not rise with the increase in transmission power of small cells. In that case, the throughput of small cells will not have a significant increase.

Figure 8 illustrates the relationship between the IB-FD network throughput and the different UE density. From Figure 8, it is obvious that the network throughput increases with the rise in C_b. Moreover, it is easy to see that the network throughput has a limitation. There are some inconsistencies among the theoretical and simulation results in Figure 8, especially for increased UE density. The main reason is that the Laplace transform of interference from small cells and macrocells has a slight difference with simulation ones for the IBFD approach.

Figures 9 and 10 compare the network throughput performance of IB-FD and OB-FDD when $C_b = 2 \times 10^6$ and $C_b = 6 \times 10^6$. It can be seen that the IB-FD approach outperforms OB-FDD, especially with a higher UE density ($>1 \times 10^{-3}$), which is because for the IB-FD approach, UEs have a relatively higher data rate because more bandwidth will be allocated to UEs for transmission with the IB-FD approach. Moreover, both OB-FDD and IB-FD have a significant improvement to the original base, especially with a small C_b.

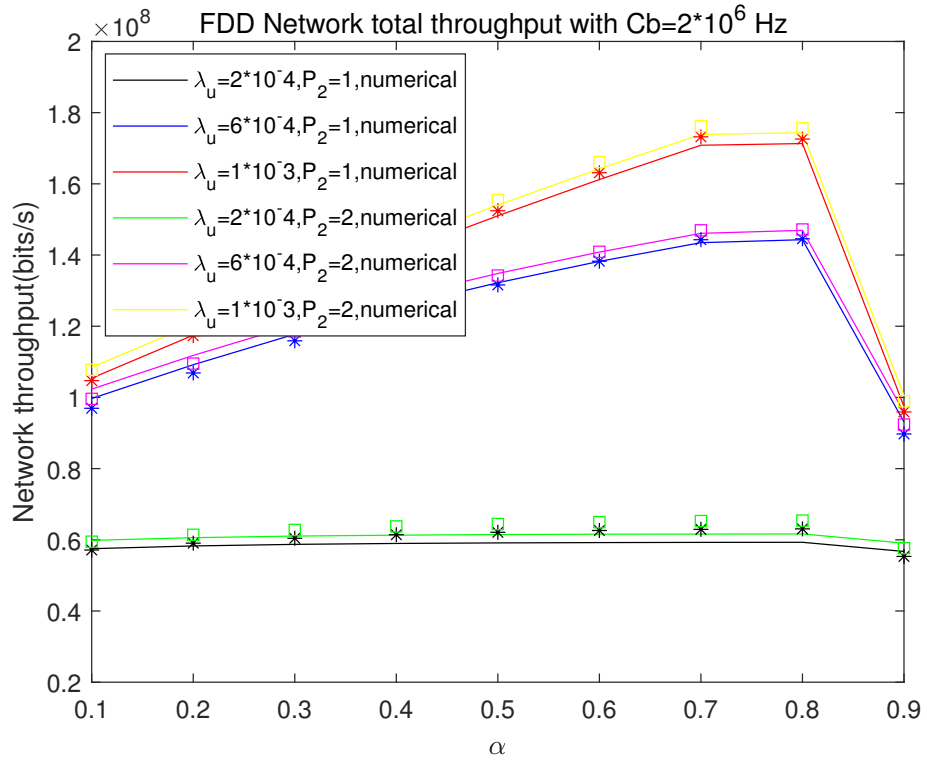

Figure 6. Network throughput with Cb = 2×10^6 based on OB-FDD.

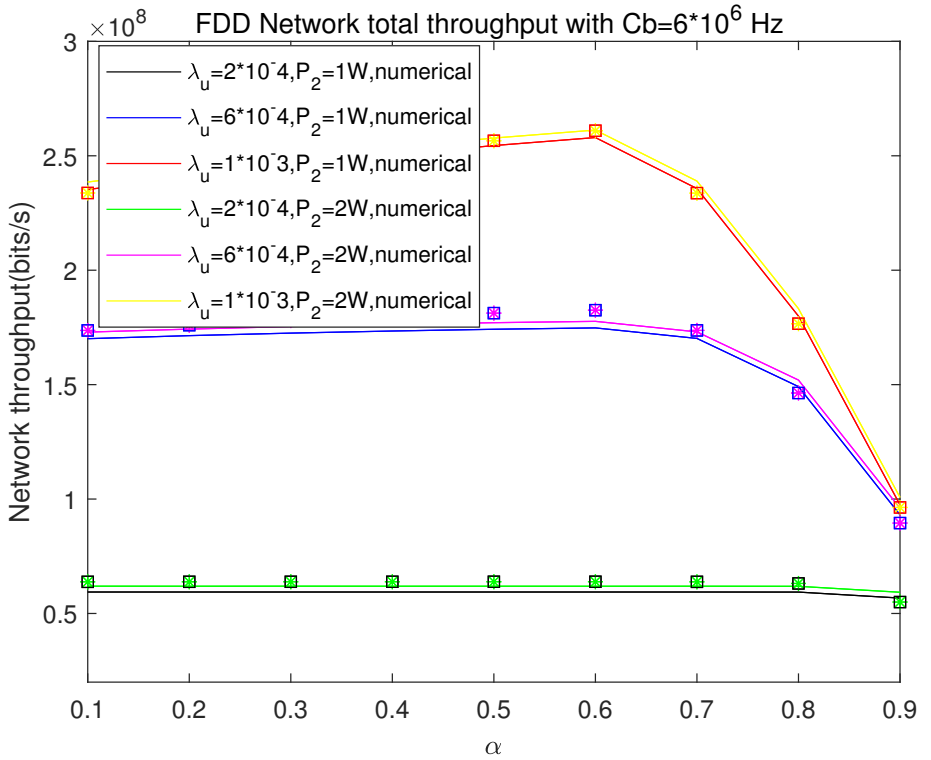

Figure 7. Network throughput with Cb = 6×10^6 based on OB-FDD.

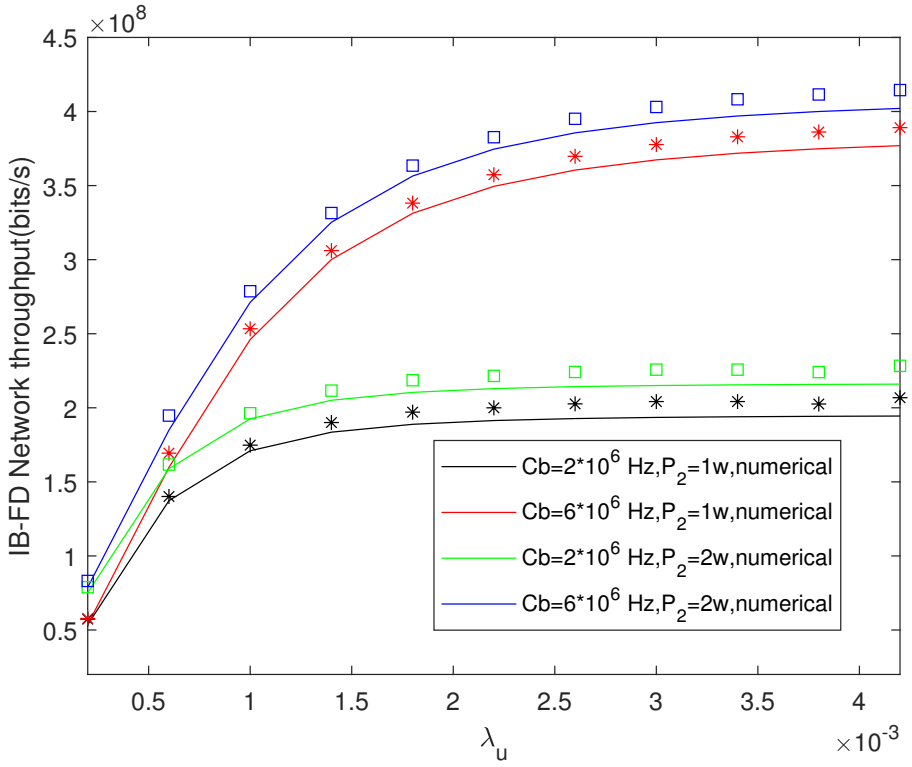

Figure 8. Network throughput with different UE density based on IB-FD.

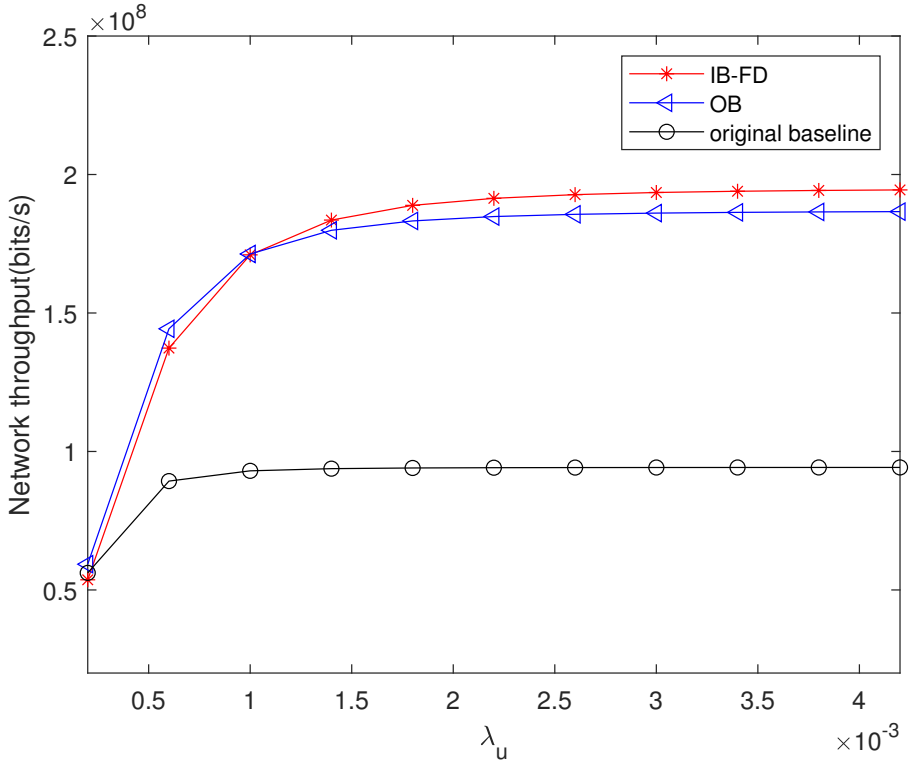

Figure 9. Network throughput with Cb = 2×10^6.

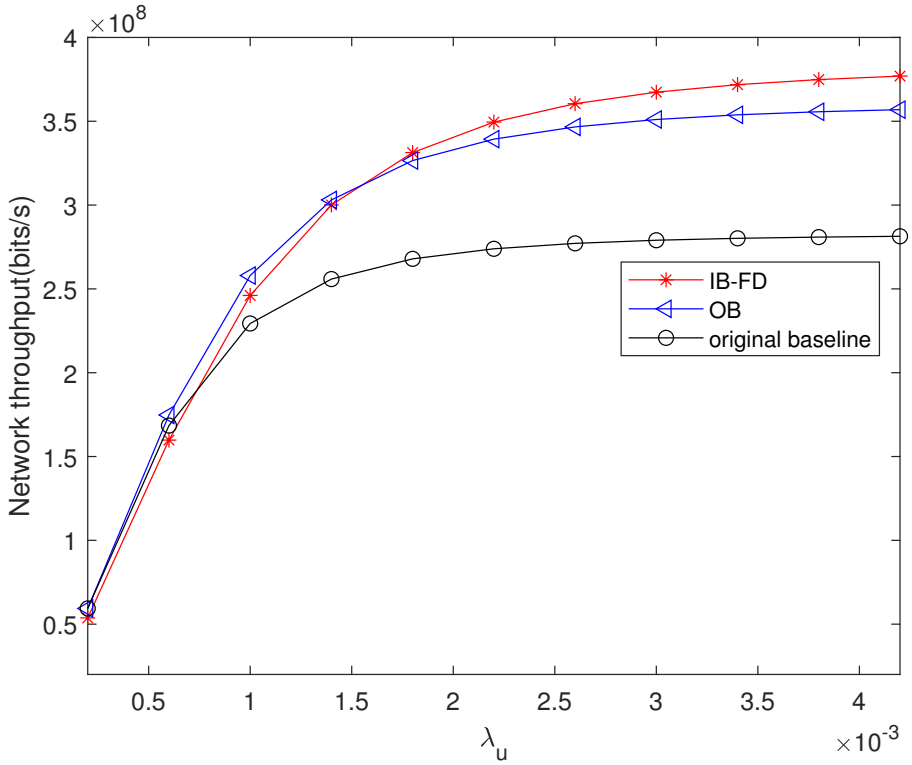

Figure 10. Network throughput with Cb = 6×10^6.

4. Conclusions

In this paper, a strategy to utilize the wireless backhaul to maximize the small cell throughput is proposed. Using a stochastic geometry-based network model, we provide a numerical analysis of the throughput of the heterogeneous networks. The results show that both the IB-FD and the OB-FDD approaches achieve much better network throughput performance than that of the original method without wireless backhaul, especially with a lower capacity of wired backhaul. We also provide a comparison between the IB-FD and OB-FDD methods. OB-FDD can be a much more suitable choice to provide a wireless backhaul for small cells close to the macrocell. Furthermore, IB-FD can achieve a higher throughput of the HetNet, especially when the UE density is high.

In real-world scenarios, especially for the urban landscapes, the integrated access and backhaul can be treated as a promising solution to address the issue of a high capacity demand. One of the main challenges in deploying wireless backhaul is to ensure a line-of-sight (LOS) transmission environment for wireless backhaul links. The need for an LOS backhaul link is critical in urban environments [24]. One of the potential strategies to address this issue is to deploy a reconfigurable intelligent surface (RIS) to help build the LOS transmission environment for wireless backhaul links. Thus, evaluating the performance of RIS-aided wireless backhaul networks is a critical problem to investigate in the future.

Author Contributions: Conceptualization, Ran Tao; methodology, Ran Tao; software, Ran Tao; validation, Ran Tao and Wuling Liu; resources, Ran Tao; writing—original draft preparation, Ran Tao; writing—review and editing, Ran Tao and Wuling Liu; supervision, Wuling Liu; funding acquisition, Ran Tao. All authors have read and agreed to the published version of the manuscript.

Funding: This research was funded by the Startup Foundation for Introducing Talent of NUIST with grant number 1523142301309.

Data Availability Statement: Dataset available on request from the authors.

Conflicts of Interest: The authors declare no conflicts of interest.

References

1. Hwang, I.; Song, B.; Soliman, S.S. A holistic view on hyper-dense heterogeneous and small cell networks. *IEEE Commun. Mag.* **2013**, *51*, 20–27. [CrossRef]
2. Abdelmoaty, A.; Naboulsi, D.; Dahmany, G.; Gagnon, F. When Resiliency Matters: An Overview of 5G and Beyond Wireless Backhaul Network Design. *IEEE Commun. Mag.* **2023**, *61*, 206–212. [CrossRef]
3. Tezergil, B.; Onur, E. Wireless backhaul in 5G and beyond: Issues, challenges and opportunities. *IEEE Commun. Surv. Tutorials* **2022**, *24*, 2579–2632. [CrossRef]
4. Li, B.; Zhu, D.; Liang, P. Small cell in-band wireless backhaul in massive MIMO systems: A cooperation of next-generation techniques. *IEEE Trans. Wirel. Commun.* **2015**, *14*, 7057–7069. [CrossRef]
5. Zhang, H.; Liu, H.; Cheng, J.; Leung, V.C. Downlink energy efficiency of power allocation and wireless backhaul bandwidth allocation in heterogeneous small cell networks. *IEEE Trans. Commun.* **2017**, *66*, 1705–1716. [CrossRef]
6. Rezaabad, A.L.; Beyranvand, H.; Salehi, J.A.; Maier, M. Ultra-dense 5G small cell deployment for fiber and wireless backhaul-aware infrastructures. *IEEE Trans. Veh. Technol.* **2018**, *67*, 12231–12243. [CrossRef]
7. Mowla, M.M.; Ahmad, I.; Habibi, D.; Phung, Q.V. Energy efficient backhauling for 5G small cell networks. *IEEE Trans. Sustain. Comput.* **2018**, *4*, 279–292. [CrossRef]
8. Forouzan, N.; Rabiei, A.M.; Vehkaperä, M.; Wichman, R. A distributed resource allocation scheme for self-backhauled full-duplex small cell networks. *IEEE Trans. Veh. Technol.* **2021**, *70*, 1461–1473. [CrossRef]
9. Son, H.; Choi, K. Low-Power Full-Duplex Self-Backhauling. *IEEE Wirel. Commun. Lett.* **2023**, *13*, 476–480. [CrossRef]
10. Sharma, D.; Nandanwar, V. Performance of induction motor at low and high speed using model predictive control method. *Int. J. Res. Sci. Eng.* **2016**, *3*, 779–785.
11. Ge, X.; Pan, L.; Tu, S.; Chen, H.H.; Wang, C.X. Wireless Backhaul Capacity of 5G Ultra-Dense Cellular Networks. In Proceedings of the 84th IEEE Vehicular Technology Conference (VTC-Fall), Montreal, QC, Canada, 18–21 September 2016; pp. 1–6.
12. Dhillon, H.S.; Caire, G. Wireless backhaul networks: Capacity bound, scalability analysis and design guidelines. *IEEE Trans. Wirel. Commun.* **2015**, *14*, 6043–6056. [CrossRef]
13. Elbayoumi, M.; Ibrahim, M.; Elhoushy, S.; Hamouda, W.; Youssef, A. Performance Analysis of Cellular Ultra Dense IoT Networks with Wireless Backhauls. *IEEE Internet Things J.* **2023**, *10*, 15774–15787. [CrossRef]
14. Tran, Q.H.; Duong, T.M.; Kwon, S. Load Balancing for Integrated Access and Backhaul in mmWave Small Cells. *IEEE Access* **2023**, *11*, 138664–138674. [CrossRef]
15. Guo, Z.; Niu, Y.; Mao, S.; He, R.; Wang, N.; Zhong, Z.; Ai, B. Joint Design of Access and Backhaul in Densely Deployed MmWave Small Cells. *IEEE Trans. Veh. Technol.* **2023**, *72*, 14498–14515. [CrossRef]
16. Lee, J.; Choi, H.H.; Lim, S.C.; Kim, H.; Na, J.; Lee, H. Low-complexity Q-learning for Energy-aware Small-cell Networks with Integrated Access and Backhaul. *IEEE Access* **2023**, *11*, 121529–121538. [CrossRef]
17. Zheng, G.; Wen, M.; Chen, Y.; Wu, Y.C.; Poor, H.V. Joint Transmit Precoding and Rate Allocation for Rate-Splitting Multiple Access Based Wireless Backhaul HetNets. In Proceedings of the ICC 2023—IEEE International Conference on Communications, Dalian, China, 10–12 August 2023; pp. 2105–2110.
18. Siddique, U.; Tabassum, H.; Hossain, E. Downlink Spectrum Allocation for In-Band and Out-Band Wireless Backhauling of Full-Duplex Small Cells. *IEEE Trans. Commun.* **2017**, *65*, 3538–3554. [CrossRef]
19. Andrews, J.G.; Baccelli, F.; Ganti, R.K. A tractable approach to coverage and rate in cellular networks. *IEEE Trans. Commun.* **2011**, *59*, 3122–3134. [CrossRef]
20. Proakis, J.G.; Salehi, M. *Digital Communications*; McGraw-Hill Higher Education: New York, NY, USA, 2007.
21. Kang, X.; Liang, Y.C.; Nallanathan, A.; Garg, H.K.; Zhang, R. Optimal power allocation for fading channels in cognitive radio networks: Ergodic capacity and outage capacity. *IEEE Trans. Wireless Commun.* **2009**, *8*, 940–950. [CrossRef]
22. Brent, R.P. *Algorithms for Minimization without Derivatives*; Prentice-Hall Series in Automatic Computation; Prentice-Hall: Englewood Cliffs, NJ, USA, 1973.
23. Jo, H.S.; Sang, Y.J.; Xia, P.; Andrews, J.G. Heterogeneous cellular networks with flexible cell association: A comprehensive downlink SINR analysis. *IEEE Trans. Wirel. Commun.* **2012**, *11*, 3484–3495. [CrossRef]
24. Ronkainen, H.; Edstam, J.; Ericsson, A.; Östberg, C. Integrated access and backhaul a New Type of Wireless Backhaul in 5G. *Ericsson Technol. Rev.* **2020**, *2020*, 2–11. [CrossRef]